Korean J. Chem. Eng., 33(8), 2308-2318 (2016)
DOI: 10.1007/s11814-016-0075-9

pISSN: 0256-1115
eISSN: 1975-7220

Simulation-based optimization of gas condensate wells to mitigate the heavy hydrocarbon condensation through supercritical CO_2 injection

Jinsuk Choi*, ByungIn Choi, Jiho Lee*, and Kun Sang Lee*,†**

*Department of Earth Resources and Environmental Engineering, Hanyang University,
222 Wangsimni-ro, Seongdong-gu, Seoul 04763, Korea
**Computer Modelling Group Ltd., Building @12, Office 320, P. O. Box 500 446, Dubai International City, Dubai, UAE
(*Received 21 June 2015 • accepted 10 March 2016*)

Abstract−In gas-condensate reservoirs suffering from condensate banking, the supercritical CO_2 injection process is regarded as one of the most effective technical remedies to reduce the liquid formation and achieve higher quality gas production. With proper well configuration and spacing designs, the injected CO_2 can decrease the loss of heavy components effectively. The main goal of this study was to minimize the loss of heavy components during CO_2 injection by implementing a proper well configuration. The results show that the integration of pressure maintenance and chemical reactions, including reduced viscosity and interfacial tension, improves the C_{7+} component recovery by 42.9, 49.4, and 49.3% for the base five-spot, inverted five-spot, and line drive cases, respectively. The total recovery is the highest for the line drive pattern with a recovery factor of 72.7%. The results also indicate that there is a critical length maximizing the effect of gas cycling.

Keywords: Gas-condensate, Gas-relative Permeability, Supercritical CO_2 Injection, Heavy Hydrocarbon, Well Configuration

INTRODUCTION

Condensate banking, which is a production problem in the development of natural gas reservoirs, occurs after a short period of production as a result of pressure drop below the dew point. As the condensate saturation increases, the gas relative permeability decreases and the productivity of the well decreases. Accumulated condensate banking at the near wellbore area can cause damage in the formation as well as a decrease of the well productivity [1-3]. The prediction of condensate banking problems and their solutions strongly depends on accurate modeling and assessment. Without proper investigation, building up of condensate in the gas reservoirs could result in potential problems because there is always the possibility of overestimating or underestimating reservoir production performance [4,5]. Condensate banking also leads to an unexpected loss of flow. Since fulfilling contractual obligations is critical in the gas industry, an inconsistent gas supply can cause undesired situations. Recently, reported problems have provoked a dramatic increase of investigations involving technical solutions [2,6-9].

One of the most effective techniques to minimize the problems caused by condensate banking is carbon dioxide (CO_2) injection [10,11]. CO_2 injection is common for pressure maintenance purposes. Pressure maintenance is economically justified by keeping the reservoir pressure above the dew point and re-vaporizing any valuable condensate that may have formed. Kurdi [11] found that the injection of supercritical CO_2 increases the density of gas, decreases the viscosity and density of condensate, and reduces the surface tension between the gas and condensate phases to lower capillary pressure. As a result, the residual condensate saturation decreases and condensate recovery increases. According to Zick [12], the combination of a condensing-vaporizing gas drive mechanism is the controlling phenomenon for the CO_2 EOR process. However, actual simulation runs based on his studies indicate that the traditional condensing-vaporizing concept does not occur in many cases. To improve the efficiency of CO_2, supercritical CO_2 injection was proposed [9,13-16]. Above the minimum miscibility pressure (MMP), the injection of supercritical CO_2 (above 7,380 kPa, 87.8 °C) leads to enhancement of the displacement efficiency by a condensing-vaporizing mechanism. The beneficial achievements can be verified based on both mechanisms; reduction of the interfacial tension and condensate viscosity.

In gas-condensate fields undergoing natural depletion, gas and condensate recovery is essentially independent of the well spacing if sufficient wells have been drilled to penetrate all productive zones. However, investigating the effects of the well configuration and well spacing on the gas-condensate reservoir productivity is a primary step. Liu [17] determined that the anisotropy of reservoir permeability has significant impacts on well pattern and reservoir exploitation results. Proper well designs are capable of determining the value of accelerated income in the natural depletion of gas-condensate reservoirs, indicating that the overall profit from gas-condensate development can be maximized depending on the well design scenario.

The main objective of this study was to quantify the effect of CO_2 cycling on the enhancement of gas-condensate productivity by analyzing interactions between injected CO_2 and the fluid in the reservoir. We also investigated the changes of the condensate composition due to several mechanisms. The primary aim was to derive

†To whom correspondence should be addressed.
E-mail: kunslee@hanyang.ac.kr

optimal well design scenarios based on supercritical CO_2 injection to minimize the loss of valuable heavy components, C_{7+}. The loss of heavy components requires additional cost to maintain the heat value of the gas supplied. Furthermore, these liquid rich heavy ends are more valuable because of current low gas prices. Prevention or delay of the loss of valuable components resulting from condensate build-up should be thoroughly analyzed in the prediction of the performance of proposed treatments in field-scale reservoirs. Considering the effects of compositional change in a heterogeneous reservoir, this study provides insight into optimization on the field-scale. Reservoir heterogeneity affects the injection performance significantly. Since gas mobility is high, the injected gas tends to flow preferentially through the high permeable path causing early breakthrough and poor sweep. It results in less effective performance with low hydrocarbon recovery. To reflect the effect of heterogeneity more realistically, a field-scale model needs to be applied. Three-dimensional simulation studies were conducted to quantify the sweep efficiencies and improvement of hydrocarbon recovery for different well pattern scenarios. In addition, optimum well spacings for the given scenarios were evaluated based on economic analysis in the field-scale reservoir model.

MATHEMATICAL FORMULISM

1. Governing Equations

The Peng-Robinson equation of state (EOS) can be tuned to characterize the fluid of the reservoirs [18]. A cubic equation of state follows:

$$p = \frac{RT}{v-b} - \frac{a}{v^2+2vb-b^2} \tag{1}$$

For mixtures, the parameters a and b are defined by the following mixing rule.

$$a = \sum_i \sum_j x_i x_j a_{ij} \tag{2}$$

$$a_{ij} = (1-d_{ij})\sqrt{a_i}\sqrt{a_j} \tag{3}$$

$$b = \sum_i x_i b_i \tag{4}$$

where x_i is the mole fraction in phase L and d_{ij} is the empirically determined interaction coefficient.

The components in each phase can be expressed by using the continuity equation.

$$\frac{\partial}{\partial t}\left[\phi\sum_{j=1}^{N_p}\rho_j S_j \omega_{ij} + (1-\phi)\rho_s \omega_s\right] + \nabla\cdot\left[\sum_{j=1}^{N_p}(\rho_j \omega_{ij}\mathbf{u}_j - \phi S_j \rho_j \mathbf{K}_{ij}\cdot\nabla\omega_{ij})\right] = \phi\sum_{j=1}^{N_p} S_j r_{ij} + (1-\phi) r_{is} \tag{5}$$

where S_j is saturation of the j phase, ω_j is the mass fraction of component i in the j phase, $\mathbf{K}_{ij}$ is the dispersion of component i in the j phase, r_{ij} is the reaction of component i in the j phase, and $\mathbf{u}_j$ is the Darcy velocity calculated by using the following equation:

$$\mathbf{u} = -\frac{k}{\mu}(\nabla p + \rho \mathbf{g}) \tag{6}$$

2. Interfacial Tension Reduction

For multicomponent systems, the interfacial tension, σ, is calculated through the Macleod-Sugden correlation [19]:

$$\sigma^{\frac{1}{4}} = \sum_{i=1}^{N_c} p_{ar_i}(x_i\rho_L - y_i\rho_V) \tag{7}$$

where y_i is the mole fraction in phase V and p_{ar} is temperature-independent parameter parachor. It is a weak function of temperature for a variety of fluids and within wide ranges of temperature.

3. Condensate Viscosity Correlation

In the compositional reservoir simulation of miscible gas injection and depletion of near-critical reservoir fluids, the oil and gas compositions can be almost similar. A single viscosity relation consistent for both phases is desired [20]. The Jossi-Stiel-Thodos approach can be used as a viscosity correlation for nonpolar fluids in the dense gaseous and liquid phase regions under reservoir condition, which is applicable in the range of $0.1 \le \rho_r < 3$ [21]. The method ensures that the viscosities of both gas and condensate converge to the same value when the pressure approaches the critical point.

$$[(\mu-\mu^*)\xi + 10^{-4}]^{1/4} = 0.1023 + 0.023364\rho_r + 0.0058533\rho_r^2 - 0.040758\rho_r^3 + 0.0093324\rho_r^4 \tag{8}$$

where μ^* is the low pressure viscosity of the mixture and ρ_r is the reduced mixture density defined as follows:

$$\rho_r = \rho v_{c\mu} = \rho\left(\sum_{i=1}^{N_c} x_i v_{c\mu_i}^{\alpha}\right)^{1/\alpha} \tag{9}$$

where $v_{c\mu}$ is the critical molar volume, which is identical to the critical volume of the component. The mixture viscosity parameter, ξ, is given as follows:

$$\xi = \frac{\left(\sum_i x_i T_{c_i}\right)^{1/6}}{\left(\sum_i x_i MW_i\right)^{1/2}\left(\sum_i x_i p_{c_i}\right)^{2/3}} \tag{10}$$

Because CO_2 density of is less than condensate, liquid density decreases with CO_2 injection leading to condensate viscosity reduction [11].

MODEL DESCRIPTION

A 3D field-scale model consisting of an anticline structure with a size of 62,225×41,012×355 m^3 was considered. To analyze the drainage area in detail, a sub-domain with a size of 2,829×2,298×33 m^3 was extracted. Fig. 1 shows the original model and subdomain extracted for the simulation study. The reservoir is located at a depth of 2,752 m from the surface, with 84% of gas filled in. The average porosity of the reservoir is 0.19 and the average permeability has a comparably low value of 5.23×10^{-3} μm^2. Permeability distribution is also illustrated in Fig. 1. The initial reservoir pressure is 34,474 kPa, which is higher than the dew point of the fluid at the initial reservoir temperature of 204 °C. All the reservoir properties are presented in Table 1.

Fluid composition data from a study by Izuwa and Obah [22] was used to generate the fluid model. As shown in Table 2, the

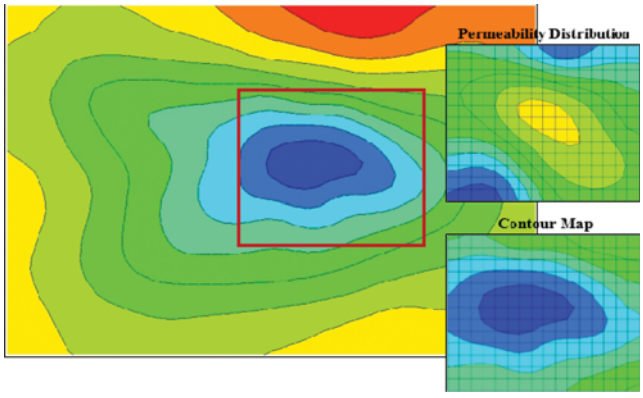

Fig. 1. 3D field-scale model evaluated in the simulation study and specific domain separated from the original region.

Table 1. Reservoir properties used for the reservoir model

Properties (Unit)	Values
Grid size (m^3)	2,829×2,298×33
Depth (m)	2,752
Average porosity	0.19
Average permeability (μm^2)	5.23×10^{-3}
Temperature (°C)	204
Initial pressure (kPa)	34,474
Initial gas saturation	0.84

Table 2. Fluid composition used in the fluid model

Components	Molecular weight	Composition (mole%)
N_2	28.01	0.24
CO_2	44.01	1.00
CH_4	16.04	69.40
C_2H_6	30.07	6.39
C_3H_8	44.10	4.98
IC_4	58.12	1.36
NC_4	58.12	2.07
IC_5	72.15	0.98
NC_5	72.15	0.79
C_6	86.20	1.39
C_{7+}	168.50	11.40

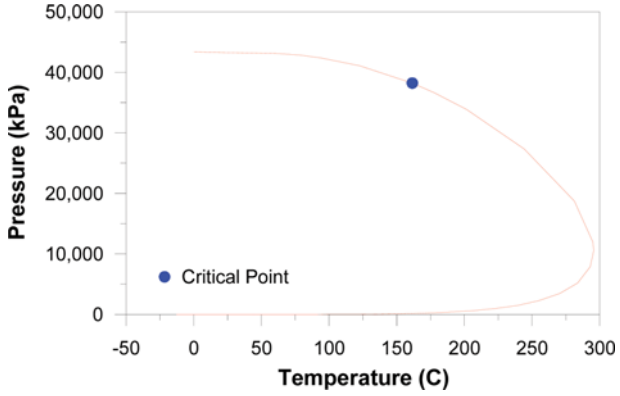

Fig. 2. Phase envelope of the gas-condensate fluid model.

fluid is mainly composed of 69.40 mole% methane and also contains heavy components, C_{7+}. To reduce the simulation time, the heavy components in the reservoir fluid are lumped into the C_{7+} component group. Fig. 2 shows the phase behavior of this fluid. The critical pressure and temperature for the fluid were determined by using the Heidemann and Khalil method [23] as 38,222 kPa and 161.5 °C, respectively.

We divided the well configuration schemes into three different cases: base five-spot, inverted five-spot, and line drive cases. Fig. 3 illustrates the flow behaviors of the different well configurations for each case. Well locations were selected with considering typical well spacing in gas-condensate reservoir. In addition, all wells were placed near the outer boundary of gas bank and distance to the aquifer was also considered to avoid early water breakthrough. The base five-spot model consists of four injectors surrounding one producer at the center. The inverted five-spot model is composed of one injector at the center surrounded by four producers. For both base and inverted five-spot cases, injector-producer well spacing ranges from 3,000 to 3,700 m. Three injectors are parallel to two producers in the line drive case, where injector-producer well spacing ranges from 4,800 to 5,200 m. Although the typical line drive case has the same number of producers and injectors, two producers are used to keep the number of wells the same as in the other cases, which is directly related to the drilling cost.

In all cases, the total production rate was set as 283,168 m^3/day and the total injection rate was the same as the production rate. Since each case has different numbers of injectors and producers,

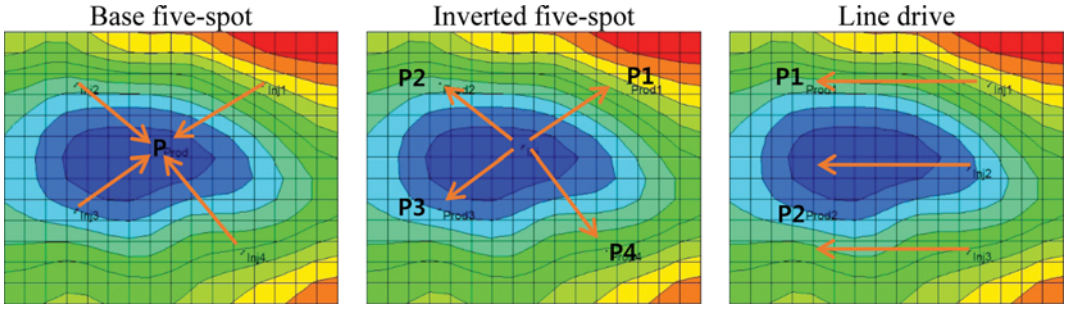

Fig. 3. Flow behavior of the injected supercritical CO_2 for the different well configurations.

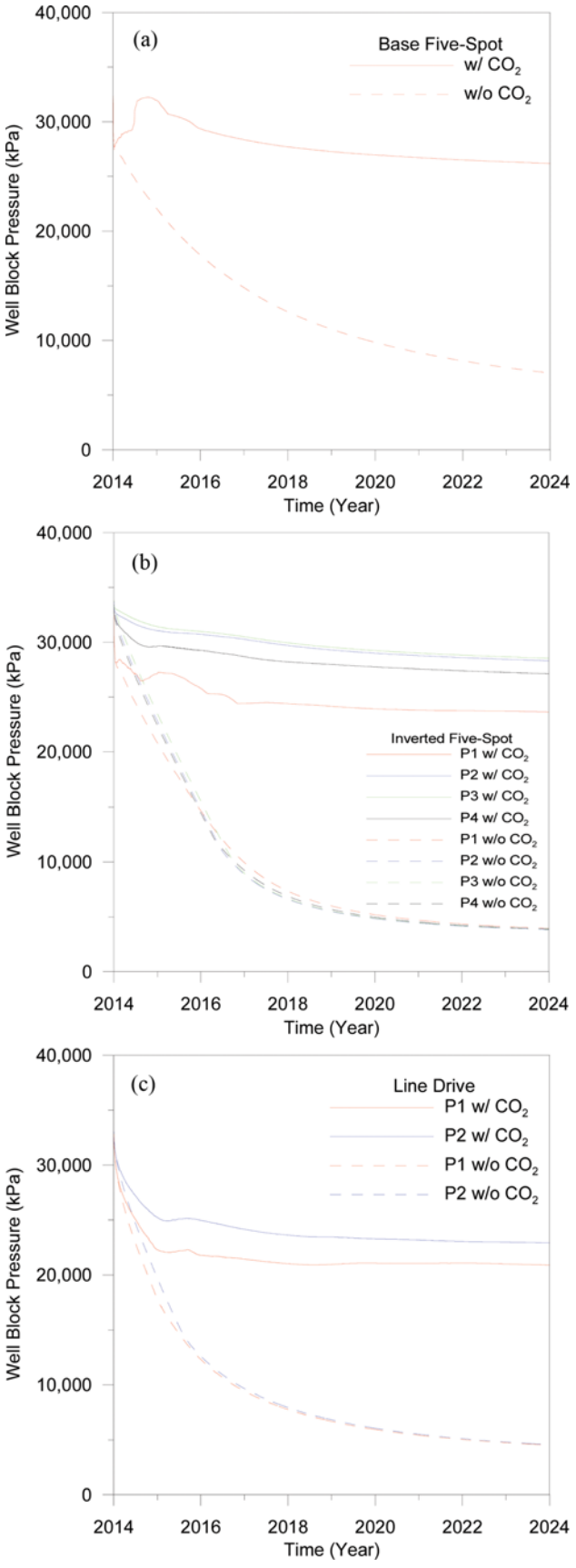

Fig. 4. Well-block pressure with and without CO_2 injection: (a) Base five-spot, (b) inverted five-spot, (c) line drive.

the total rate was equally allocated into the producers and injectors for each case. The entire operation time simulated was ten years.

RESULTS AND DISCUSSION

1. Pressure Maintenance

For the main purpose of gas cycling, reservoir pressure maintenance is a critical issue. Gas cycling aims to keep the pressure higher than the dew point of the gas in the reservoir. As a result, any liquid condensate which may have been formed is revaporized to the gas phase to prevent the condensation of valuable heavy components [24]. However, it is very hard to re-vaporize condensed liquid because the condensed liquid phase and uncondensed gas phase segregate after condensation, and this phase separation dramatically slows the reverse process of recombining gas and liquid [25].

As shown in Fig. 4, the pressures in the CO_2 injected cases are higher than those in the non-CO_2 injected cases in all well configurations. The injected CO_2 maintains the pressure and mitigates the production reduction effect. For the base five-spot case illustrated in Fig. 4(a), the pressure decreased by 7,019 kPa, whereas the injection of CO_2 maintained the pressure up to 26,200 kPa throughout the operation period. The sudden rise of the pressure over ten months is caused by four injectors surrounding the producer. This is because fewer space blocks spreading the pressure decline, and it can be considered to be more effective from a pressure maintenance perspective. After CO_2 breakthrough, the pressure starts to decline again, similar to the other cases. In the inverted five-spot case, the pressure around the producers was 3,999 kPa after ten years of production. The pressures in the producer well-blocks were maintained up to 28,269 kPa when CO_2 was injected for ten years. This shows that injection of CO_2 by a single injector can possibly support the pressures of four producers. The well-block pressure dwindled from 34,474 to 4,509 kPa with production in the line drive case and CO_2 injection increased the pressure up to 22,911 kPa, as exhibited in Fig. 4(c).

Fig. 5 shows the pressure distribution over time for the base five-spot case. The pressure drop extends over a wide range of the reservoir, and there is a particularly sharper and larger drop in the near wellbore region. Without CO_2 injection, the pressure continuously decreased from the wellbore to the outer boundary of the reservoir and the pressure at the well-block decreased to 21,000 kPa from the initial value of 34,474 kPa after 500 days of production. On the other hand, a pressure increment at the outer boundary and less drop in the near wellbore region are observed while maintaining the well-block pressure up to about 30,000 kPa with CO_2 injection.

The time for CO_2 breakthrough differed from case to case. Since CO_2 breakthrough causes a large portion of CO_2 to be produced and lowers the hydrocarbon gas fraction, the delay of CO_2 breakthrough can be a substantially important factor to validate the effectiveness of the CO_2 cycling process. Fig. 6 shows the time for CO_2 to reach each producer in the various well configurations. The time when well block CO_2 saturation exceeded 0.2 was considered as breakthrough time. The average time to breakthrough is the shortest in the inverted five-spot case with a value of 8.5 months followed by the base five-spot and line drive cases with values of 10

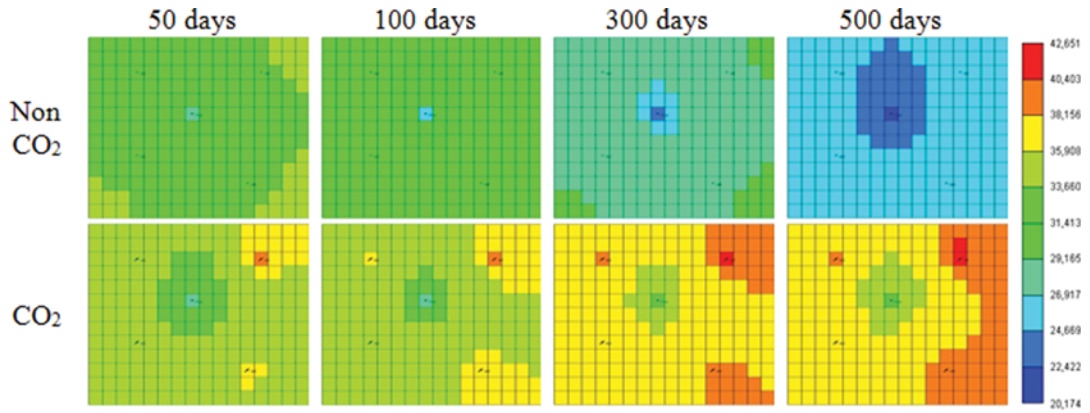

Fig. 5. Reservoir pressure distributions over time with and without CO_2 injection (kPa) in base five-spot case.

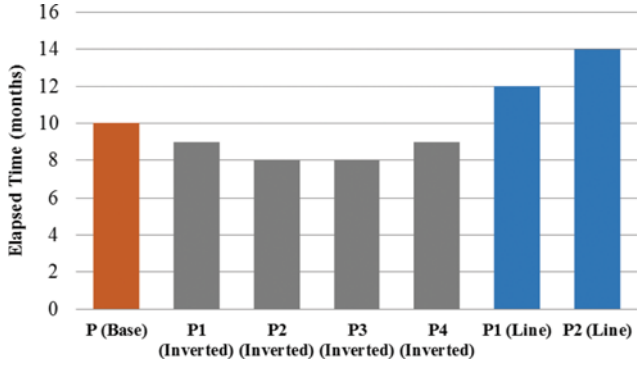

Fig. 6. CO_2 breakthrough times at each producing well for the various well configurations.

and 13 months, respectively.

Because of the constant rate condition of the producers, there are no big differences in the total gas production. However, the hydrocarbon gas rates are different in terms of quantity. As illustrated in Fig. 7, the sum of the gas phase moles excluding CO_2 from each producer shows a lower production rate at the initial stage. This is because condensate formed near the wellbore is flooded by the injected CO_2. The flooded condensate lowers the relative gas permeability and decreases gas production. Later, the condensate volume drops with pressure maintenance and the gas rate should be restored. However, the gas mole rate decreases consistently because of CO_2 breakthrough. The production condition keeps producing gas at a constant rate, but the high CO_2 mole fraction in the produced gas phase lowers the hydrocarbon gas recovery in all cases with values over 70% 4 years after injection. Overall, production rate reaches a plateau after breakthrough. However, the base case does not show the same trend. By setting total production rate the same as total injection rate through four different injectors, production rate is four-times greater than injection rate in the base case. Therefore, the pressure near producer decreases rapidly at initial stage. When injected CO_2 surrounds the producer well block, the pressure recovers significantly, resulting in de-condensation and increased gas recovery due to less space to spread as mentioned above. Thus, the base case does not reach plateaus at breakthrough time even though CO_2 mole fraction increases steadily at near wellbore zone.

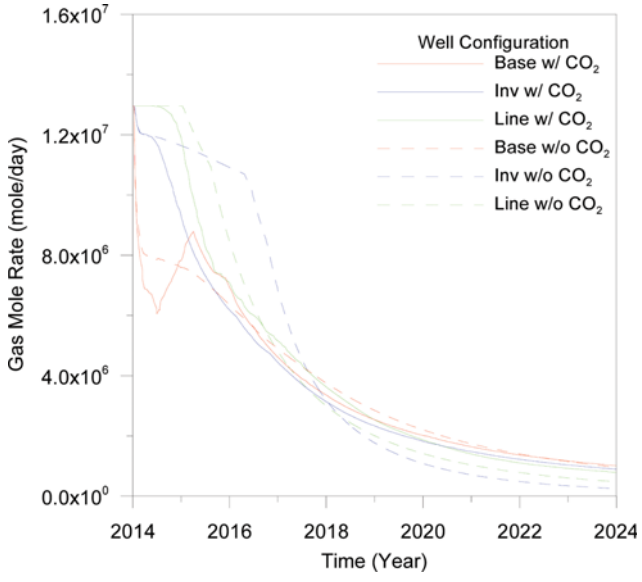

Fig. 7. Total hydrocarbon gas mole rate with and without CO_2 injection for the different well configurations.

2. Condensation Alleviation

Accumulated condensate near the wellbore region is closely related to gas flow based on the relative permeability concept. As the bottom-hole pressure drops below the dew point pressure, increased condensate saturation and decreased gas relative permeability result in less gas flow. Fig. 8 shows the condensate volume near the wellbore region for the three different cases. After CO_2 injection, the condensate formed is flooded from the outside of the wellbore, causing higher condensate saturation despite the pressure maintenance. Condensate occupies larger volume in CO_2 injected cases near the wellbore compared to non-CO_2 injected cases at initial stage. The base five-spot case exhibited a 34% increment of the condensate volume. It increased from 11 to 40% for the inverted five-spot case, and from 23 to 25% for the line drive case. As injection continues, the effect of pressure support mitigates condensate formation and, consequently, the condensate volume near the wellbore decreases significantly.

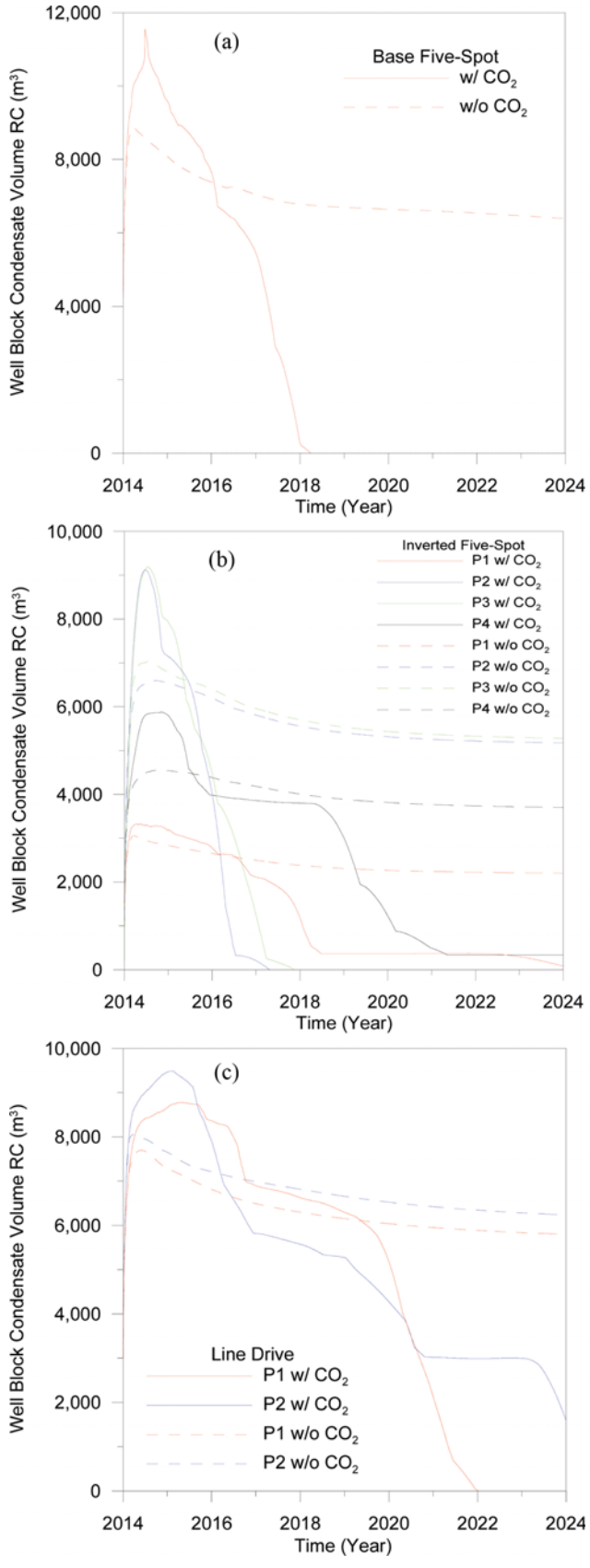

Fig. 8. Well-block condensate volumes at the reservoir condition with and without CO_2 injection: For the (a) base five-spot, (b) inverted five-spot, (c) line drive.

All cases show similar tendencies of increasing at the beginning of injection and consistently decreasing after the peak. Condensate volume reduction relies on the permeability and distance between the injector and producer. For example, in the inverted five-spot case, there are longer distances for producers 1 and 4 compared to producers 2 and 3, so that the flooding effect lasts longer. Additionally, the pore volume near each well is different and, hence, they contain different amounts of condensate.

Fig. 9 describes condensate saturation with different well patterns 50 days after production. In all cases, most of the condensation occurs near the wellbore region due to the large pressure reduction. The non-CO_2 injection cases show substantial condensation over a larger area of the reservoir, whereas CO_2 injection significantly reduces the amount of condensate formed.

Viscosity reduction is an influential effect that helps condensate to be recovered more easily. As illustrated in Fig. 10, CO_2 injection in the base five-spot patterned model reduces the condensate viscosity effectively over time, while in the non-CO_2 injected case the viscosity continuously increases. CO_2 condensing into the oleic phase makes the condensate have lower viscosity in accordance with viscosity and density mixing. This results in an enhancement of the oil phase mobility and, hence, a higher recovery of condensate can be achieved.

Fig. 11 shows the interfacial tension between the oil and gas phases. In the CO_2 non-injected case, the interfacial tension near the producer increases as production continues. Due to the pressure decrease around the producer, condensates are generated and the phases are separated. However, in the CO_2 injected case, the interfacial tension is mostly sustained because of the pressure maintenance effect.

3. Heavy Components in the Produced Gas

Since the aim of gas cycling is to not lose heavy components as a liquid phase, heavy component production in the gas phase is of critical importance to demonstrate its performance. Fig. 12 shows the gas phase mole fraction of C_{7+} components at the near wellbore region. In all cases, there is an increment of the production of gas phase C_{7+} components at the initial stage and it decreases over time. Similar to the condensate volume, a longer distance between the injector and producer causes this component to stay near the wellbore longer, as shown in Fig. 12(b).

Efficient pressure maintenance supports more C_{7+} to be produced in the base five-spot case. However, this does not mean that the base five-spot case has the best heavy component recovery. Fig. 13 illustrates the recovery factors of the C_{7+} components for each well configuration. At the end of the simulation, the C_{7+} recovery factors are 72.1%, 69.5%, and 72.7% for the base five-spot, inverted five-spot, and line drive cases, respectively. The trends of the recovery for the base five-spot and inverted five-spot cases are similar. However, early CO_2 breakthrough in the inverted five-spot case deteriorates the displacement of C_{7+} components over time. Since only one producer in the base five-spot case has to cover the effect of four producers compared to the inverted five-spot, its bottom-hole pressure decreases more rapidly until the injected CO_2 supports the pressure. Because of this effect, the bottom-hole pressure reaches the abandonment pressure within several months, causing a substantial drop of the production rate. A poor recovery was

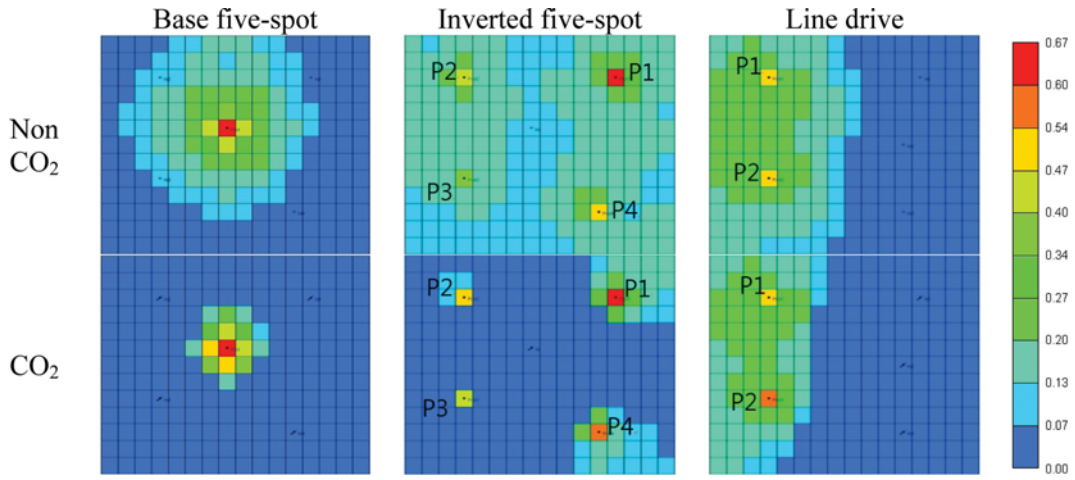

Fig. 9. Condensate saturation with and without CO_2 injection after 50 days of production.

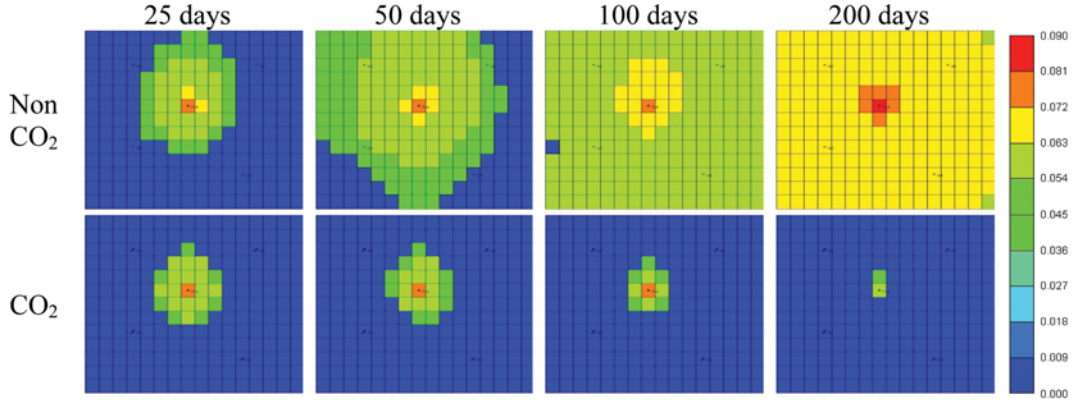

Fig. 10. Viscosity reduction of the oil phase with CO_2 injection (10^{-3} kg/m·s).

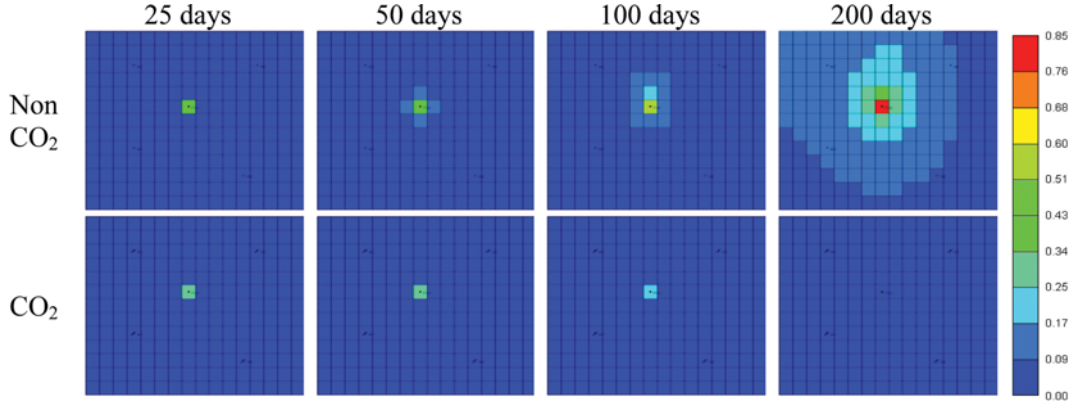

Fig. 11. Reduction of the interfacial tension by supercritical CO_2 injection over time (10^{-3} N/m).

obtained in the initial stage, but it gradually improved again due to pressure support from CO_2 injection. Much lower C_{7+} displacement was observed at the early to mid-stage for the line drive case because the distance between the injector and producer was larger than in the other cases. Since C_{7+} in the gas phase stays in the near wellbore region for a long time, long term C_{7+} recovery is possible. Eventually, the recovery factor in the line drive system overtakes the other cases at the end of the simulation.

4. Well Spacing

Since the line drive case showed the best performance in recovering heavy components after ten years, two additional cases were evaluated to examine the effect of well spacing. In one case, the injectors were shifted 305 m closer to the producer in the *x*-direction, and in the other case the injectors were moved 305 m away

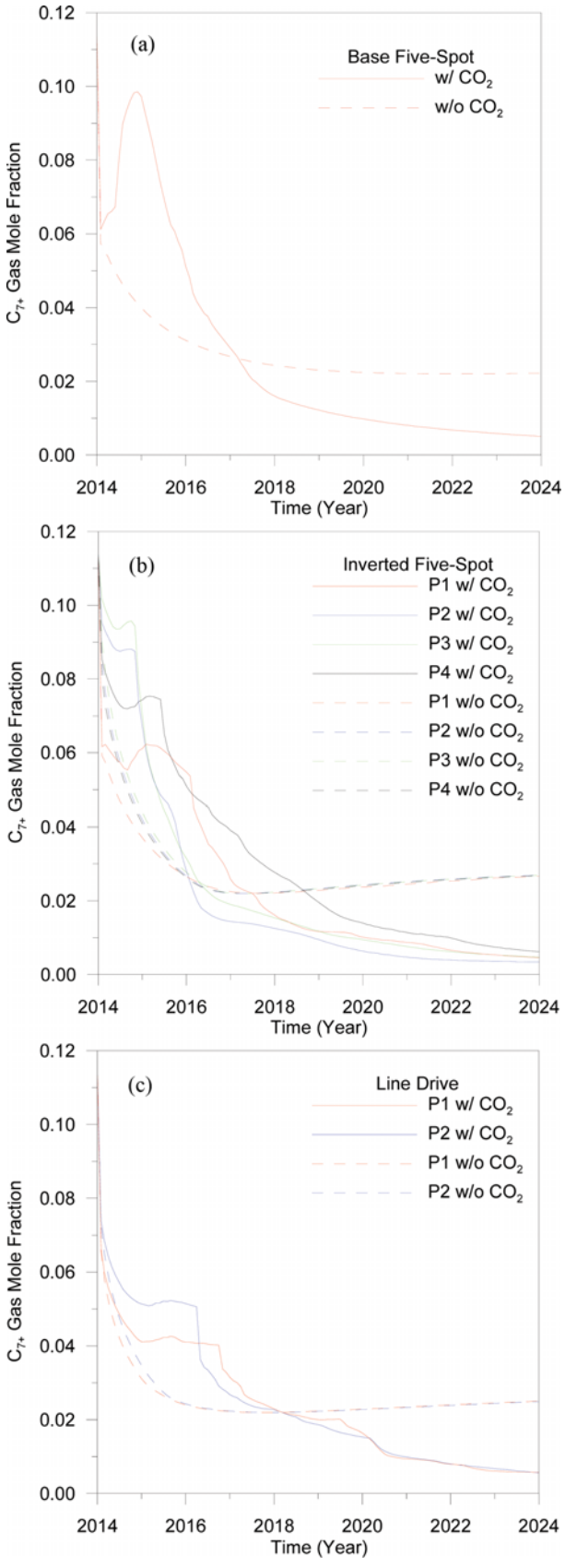

Fig. 12. C_{7+} component mole fraction in the gas phase at the producing well-block with and without CO_2 injection: (a) Base five-spot, (b) inverted five-spot, (c) line drive.

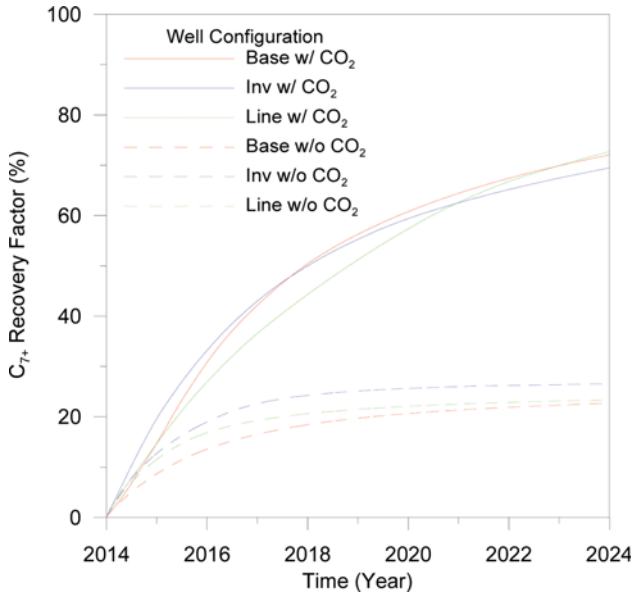

Fig. 13. C_{7+} component recovery factor with and without CO_2 injection.

from the producers. Therefore, the distances between the injectors and producer in the original well spacing, shorter spacing, and longer spacing cases are 1,585 m, 1,280 m, and 1,890 m, respectively.

The results imply that a longer distance between wells can cover a larger volume of the reservoir and make it possible to sweep more hydrocarbons. Figs. 14(a) and 14(b) show the cumulative hydrocarbon gas and condensate moles recovered in each case. With increasing well spacing, the recovery improves as well. The C_{7+} recovery factor was improved by 1.6% in the longer spacing case and declined by 3.1% in the shorter spacing case, as shown in Fig. 14(c). Shorter well spacing results in faster gas recovery at early time, but less amount of hydrocarbons and earlier breakthrough makes total recovery decreased as shown in Fig. 14(d).

The recovery is not always proportionate to the well spacing. When applying the same well spacing cases with a one-tenth volume of injected CO_2, the results are reversed, as presented in Fig. 15. This indicates that there is a critical well spacing which can maximize the recovery depending on injection and the production rate. The existence of a critical well spacing is based on the numerical results for cases considered in this study. As many other studies have mentioned the impact of well spacing, the determination of appropriate well spacing during gas injection would be still an important issue [26-28]. It is critical to analyze and determine the proper well spacing when considering gas cycling method to maximize hydrocarbon production.

CONCLUSIONS

We investigated the effects of well configuration on the recovery of heavy components from a gas-condensate reservoir by injecting supercritical CO_2 on the field-scale. The benefits and efficiency were estimated in terms of gas productivity and petrophysical characteristics. The following conclusions can be made.

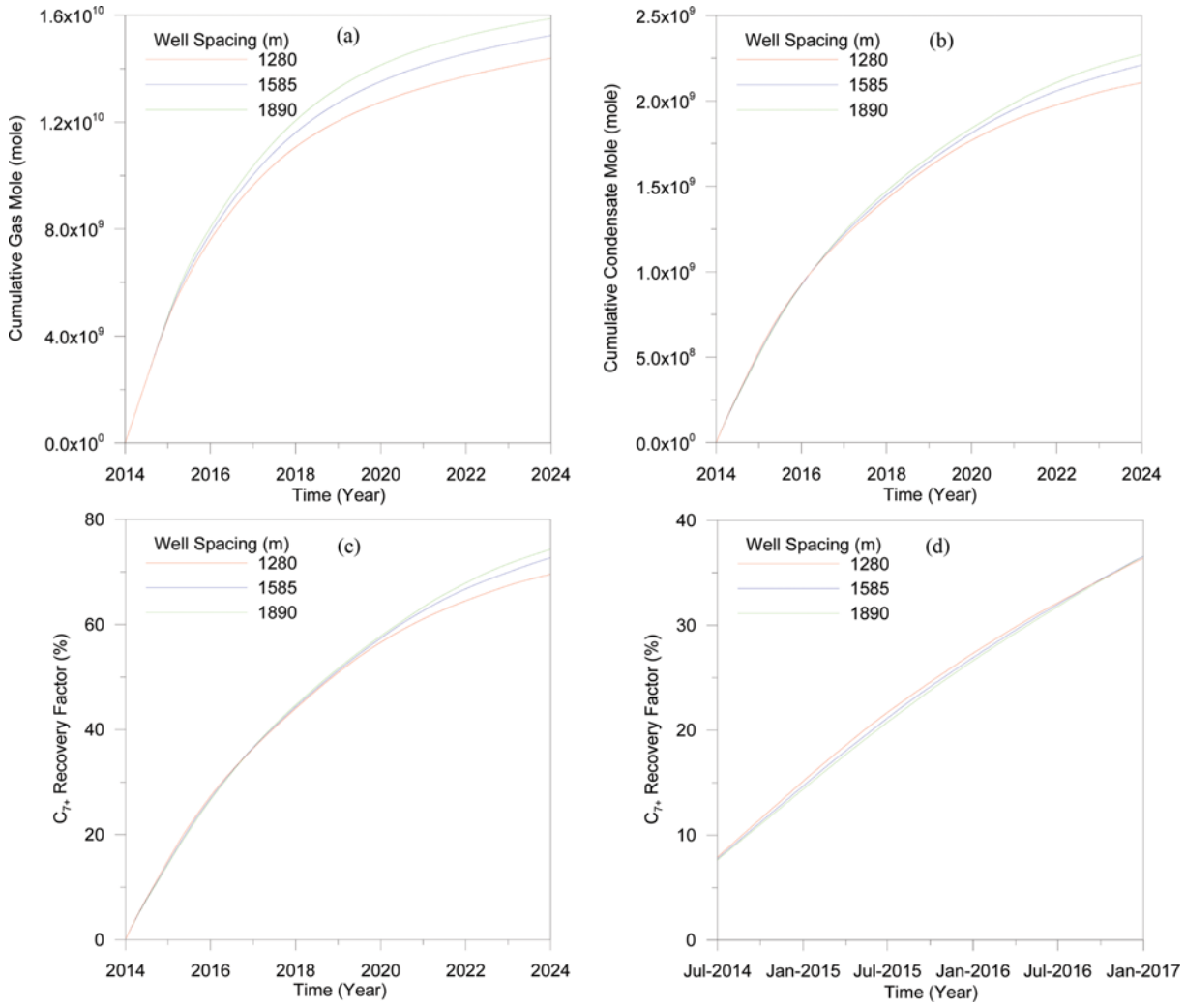

Fig. 14. Cumulative gas and condensate moles and C_{7+} recovery factors for the different well spacings in the line drive case: (a) Cumulative gas moles, (b) cumulative condensate moles, (c) total C_{7+} recovery factor, (d) total C_{7+} recovery factor at early stage.

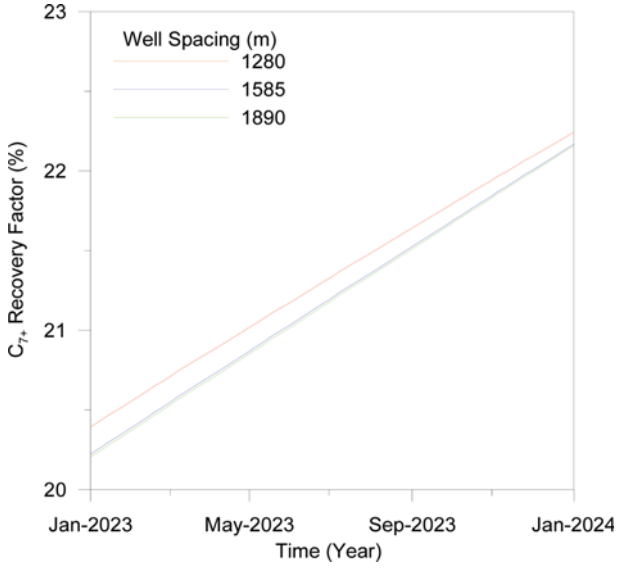

Fig. 15. C_{7+} recovery factor while injecting one-tenth of the CO_2 volume with the different well spacings in the line drive case.

1) Effective pressure maintenance reduced the condensate banking effect. However, the total amount of hydrocarbon gas moles produced decreased due to CO_2 breakthrough. The produced CO_2 mole fraction reached over 70% within four years of injection.

2) Condensate flooding at the initial stage incurred a large increment of condensate accumulation near the wellbore from 11 to 40%, but it decreased significantly over time due to pressure maintenance.

3) The heavy component (C_{7+}) recovery factors at the end of the simulations were 72.1%, 69.5%, and 72.7% for the base five-spot, inverted five-spot, and line drive cases, respectively. Because the well spacing of the line drive case is longer than the other cases, gradual and long-term production of heavy components was observed and finally, its recovery factor exceeded those of the other cases.

4) The well spacing between the injector and producer affected the CO_2 response time, condensate decrease near the wellbore, and the C_{7+} production trend. A longer distance delayed CO_2 breakthrough, curtailed condensate decreasing rate, and gradually produced C_{7+} components for a long time.

5) A longer well spacing also improved the performance of hydrocarbon displacement. However, there is a critical well spacing depending on injection and the production rate, which can maximize the effect of gas cycling according to the reversed result of the heavy component recovery factor obtained in additional cases.

ACKNOWLEDGEMENTS

This work was supported by the Energy Efficiency & Resources of the Korea Institute of Energy Technology Evaluation and Planning (KETEP) grant funded by the Korea government Ministry of Trade, Industry & Energy (MOTIE) (No. 20132010201760).

NOMENCLATURE

- a : attractive constant in the EOS
- a_{ij} : attractive constant between components i and j
- b : repulsive term constant in the EOS
- b_i : repulsive term in the EOS
- d_{ij} : empirically determined interaction coefficient
- g : gravitational acceleration [m/s^2]
- k : permeability [m^2]
- K_{ij} : dispersion of component i in phase j [m^2/s]
- MW_i : molecular weight of component i
- N_c : number of components
- N_p : number of phases
- p : pressure [atm]
- p_{ar_i} : parachor of component i
- p_{ci} : critical pressure of component i
- r_{ij} : homogeneous reaction rate of component i in phase j [g/m^3·s]
- r_{is} : reaction of solid [g/m^3·s]
- R : universal gas constant [atm·m^3/K·mole]
- S_j : saturation of phase j
- t : time [sec]
- T : temperature [K]
- T_{ci} : critical temperature of component i [K]
- u_j : darcy velocity of phase j [m/s]
- v : molar volume [m^3/mole]
- $v_{c\mu_i}$: critical molar volume used in the viscosity correlation [m^3/mole]
- x_i : mole fraction of component i in the liquid phase
- y_i : mole fraction of component i in the vapor phase
- α : mixing exponent parameter
- ϕ : porosity
- μ : fluid viscosity [kg/m·s]
- μ^* : viscosity at atmospheric pressure [kg/m·s]
- ρ_j : density of phase j [mole/m^3]
- ρ_L : molar density of the liquid phase [mole/m^3]
- ρ_r : reduced liquid density [mole/m^3]
- ρ_s : density of the solid [rock]
- ρ_V : molar density of the vapor phase [mole/m^3]
- σ : interfacial tension [N/m]
- ω_{ij} : mass fraction of component i in phase j
- ω_{is} : mass fraction of component i in the solid
- ξ : mixture viscosity parameter [m·s/kg]

REFERENCES

1. S. H. Yousefi, A. Eslamian and F. Rashidi, *Korean J. Chem. Eng.*, **31**, 1 (2014).
2. R. S. Barnum, F. P. Brinkman, T. W. Richardson and A. G. Spillette, *SPE Annual Technical Conference and Exhibition*, Dallas, Texas, October 22-25 (1995).
3. W. W. P. Wang, M. Delshad, C. Wang, G. A. Pope and M. M. Sharma, *SPE Asia Pacific Conference on Integrated Modelling for Asset Management*, Kuala Lumpur, Malaysia, March 23-24 (1998).
4. J. K. Ali, P. J. McGauley and C. J. Wilson, *SPE Annual Technical Conference and Exhibition*, San Antonio, Texas, October 5-8 (1997).
5. A. Mahbub, M. Y. Al-Qahtani and R. Zillur, *SPE Annual Technical Conference and Exhibition*, San Antonio, Texas, September 29-October 2 (2002).
6. R. M. M. Smits, N. Van der Post and S. M. Al Shaidi, *SPE Middle East Oil Show*, Bahrain, March 17-20 (2001).
7. H. A. Al-Anazi, J. R. Solares and M. Al-Faifi, *SPE Asia Pacific Oil and Gas Conference Exhibition*, Jakarta, Indonesia, April 5-7 (2005).
8. C. Shi, R. N. Horne and K. Li, *SPE Annual Technical Conference and Exhibition*, San Antonio, Texas, September 24-27 (2006).
9. J. Kamath, *J. Petroleum Technol.*, **59**, 04, 94 (2007).
10. A. S. Al-Abri and R. Amin, *SPE Annual Technical Conference and Exhibition*, New Orleans, Louisiana, October 4-7 (2009).
11. M. Kurdi, J. Xiao and J. Liu, *SPE Saudi Arabia section Young Professionals Technical Symposium*, Dhahran, Saudi Arabia, March 19-21 (2012).
12. A. A. Zick, *SPE Annual Technical Conference and Exhibition*, New Orleans, Louisiana, October 5-8 (1986).
13. B. Moradi, J. Tangsirifard, M. R. Rasaei, A. M. Maklavani and M. B. Bagheri, *Trinidad and Tobago Energy Conference*, Port of Spain, Trinidad, June 27-30 (2010).
14. H. Gachuz-Muro, B. Gonzalez-Valtierra, E. Luna-Rojero, B. Aguilar-Lopez and A.Pineda-Munoz, *SPE Enhanced Oil Recovery Conference*, Kuala Lumpur, Malaysia, July 19-21 (2011).
15. M. Soroush, L. Hoier and J. Kleppe, *18th SPE Improved Oil Recovery Symposium*, Tulsa, Oklahoma, April 14-18 (2012).
16. A. Taheri, *EAGE Annual Conference and Exhibition*, London, United Kingdom, June 10-13 (2013).
17. Y. Liu, *International Oil Conference and Exhibition*, Veracruz, Mexico, June 27-30 (2007).
18. D. Y. Peng and D. B. Robinson, *Industrial and Engineering Chemistry: Fundamentals*, **15**, 59 (1976).
19. S. Sugden, *J. Chem. Soc.*, **125**, 1177 (1924).
20. C. H. Whitson and M. R. Brulé, *Phase Behavior*, Society of Petroleum Engineers Inc. (2000).
21. J. A. Jossi, L. I. Stiel and G. Thodos, *American Institute Chem. Engineers J.*, **8**, 1 (1962).
22. N. C. Izuwa and B. Obah, *SPE Nigeria Annual International Conference and Exhibition*, Lagos, Nigeria, August 5-7 (2014).
23. R. A. Heidemann and A. M. Khalil, *American Institute Chem. Engineers J.*, **26**, 05, 769 (1980).
24. M. A. Sayed and G. A. Al-Muntasheri, *SPE International Symposium and Exhibition on Formation Damage Control*, Lafayette, Louisiana, February 26-28 (2014).
25. L. Fan, B. W. Harris, A. Jamaluddin, J. Kamath, R. Mott, G. Pope,

A. A. Shandrygin and C. H. Whitson, *Oilfield Review*, **17**, 04, 14 (2005).
26. A. Khanal, M. Khoshghadam and W. J. Lee, *SPE Liquids-Rich Basins Conference*, Midland, Texas, September 2-3 (2015).
27. V. Sahai, G. Jackson, R. Rai and L. Coble, *Americas Unconventional Resources Conference*, Pittsburgh, Pennsylvania, June 5-7 (2012).
28. F. Lalehrokh and J. Bouma, *SPE/CSUR Unconventional Resources Conference*, Calgary, Alberta, Canada, September 30-October 2 (2014).